gering of the amino lone pair and CH bonds with the cyclopropyl CH and CC bonds.

The shortening of C_1N relative to methylamine and dimethylamine is consistent with a higher degree of s character in the exocyclic cyclopropyl orbital compared to the corresponding methyl orbital. The longer NH bond is cyclopropylamine relative to other simple amines can be understood on the basis of a greater degree of pyramidalization of the amino group in the former compound (more p character in the NH bond). This increased pyramidalization is also consistent with a minimization of π'-electron repulsion between the amino lone pair and NH bonds and the cyclopropyl 3e'(S) and 3e'(A) orbitals, respectively, as discussed above.

Finally, we note that our conclusion that there is little evidence for π'-electron donation into the cyclopropyl 4e'(S) orbital (Figure 2a) is in accord with those of Boggs and co-workers,[35] who showed that the total electron density on nitrogen in cyclopropylamine indicates little dependence of charge on rotation angle, and of Compton et al.,[36] who rejected such an interaction on the basis of the similar magnitudes of the trans → gauche barriers in cyclopropylamine and isopropylamine. Interestingly, the greater enthalpy difference between the gauche conformation and the more stable s-trans conformation in cyclopropylamine relative to isopropylamine is fully consistent with a four-electron repulsion between the nitrogen lone pair and the cyclopropyl 3e'(A) orbital in the gauche conformation of the former compound.

(33) Ehrenson, S.; Brownlee, R. T. C.; Taft, R. W. *Prog. Phys. Org. Chem.* **1973**, *10*, 1.
(34) Boggs, J. E., personal communication. We thank Professor Boggs for these values.
(35) Mochel, A. R.; Boggs, J. E.; Skancke, P. N. *J. Mol. Struct.* **1973**, *15*, 93.
(36) Compton, D. A. C.; Rizzolo, J. J.; Durig, J. R. *J. Phys. Chem.* **1982**, *86*, 3746.

Summary

A complete heavy-atom microwave structure of cyclopropylamine and full 6-31G* and MP2/6-31G* geometry-optimized structures are reported. The three-membered ring structure is similar to that of cyclopropane, but there is a small but distinct shortening of C_1C_2. We attribute this primarily to hybridization changes at C_1 caused by the increased electronegativity of the amino group relative to hydrogen. Other features of the structure, such as a relatively highly pyramidal amino group which adopts a staggered perpendicular conformation with respect to the cyclopropyl ring, can be attributed to four-electron repulsive interactions between filled amino and cyclopropyl orbitals. In contrast to the key roles of hybridization and π repulsion/polarization effects, we conclude that σ-electron withdrawal from the 1e''(S) cyclopropyl orbital is of less importance and find little or no evidence for a significant role for π'-electron donation from the lone pair to the 4e'(S) cyclopropyl orbital.

Acknowledgment. This research has been supported by NSF Grant CHE 81-08395 at the University of Kansas and by NSF Grants CHE 81-10428 and 83-18188 at the University of Nebraska. We thank Douglas Tobias and Timothy Norden for assistance with the ab initio calculations.

Registry No. Cyclopropylamine, 765-30-0; cyclopropylamine-^{15}N, 103851-60-1.

Comparative Stabilities of Cationic and Anionic Hydrogen-Bonded Networks. Mixed Clusters of Water–Methanol

Michael Meot-Ner (Mautner)

Contribution from the Chemical Kinetics Division, Center for Chemical Physics, National Bureau of Standards, Gaithersburg, Maryland 20899. *Received April 14, 1986*

Abstract: The thermochemistry of the mixed water–methanol cationic clusters $(H_2O)_n(CH_3OH)_mH^+$ and anionic clusters $[(H_2O)_n(CH_3OH)_m - H]^-$ (i.e., clusters containing OH^- or CH_3O^-) was measured. The stability of the total hydrogen-bonded network in each positive cluster is greater by 3–6 kcal/mol than in the corresponding negative cluster. The variation of the stabilities of the cationic and anionic clusters with composition shows remarkable similarities. (1) Both $H_3O^+ \cdot nH_2O$ and $OH^- \cdot nH_2O$ show effects of solvent shell filling at $n = 3$. (2) Both for anions and cations, neat methanol clusters are more stable than neat water clusters. (3) Both $CH_3OH_2^+$ and CH_3O^- are solvated more strongly by methanol than by water. (4) Stepwise ion solvation compresses the differences between the gas-phase acidities of H_2O and CH_3OH and also between the gas-phase basicities. The compression effect with increasing solvation is somewhat larger in the positive than in the negative ions. (5) Both for anions and cations, stepwise replacement of H_2O by CH_3OH is exoergic for every step from neat water to neat methanol. The results indicate that in the water–methanol clusters, the favored topology places methanol molecules near the charged centers and water molecules at the periphery. This is in contrast to blocked clusters such as water–acetonitrile, where hydrogen-bonding requirements place water at the protonated center and acetonitrile at the periphery. In general, the observed trends show the significance of the formation of unlimited O–H···O hydrogen-bonded networks in both the cationic and anionic water–methanol clusters.

The stepwise clustering of neutral solvent molecules onto an ionic moiety constitutes a transition between isolated ions and electrolyte solutions. Electrolyte solutions often involve mixtures of solvents, and it is therefore important to extend clustering studies to systems which involve a mixture of components. Multicomponent clusters are also found in radiation environments such as the Earth's ionosphere. In a present series of papers we are investigating clusters of components that are used in mixed solvents and/or are found in the atmosphere such as H_2O, CH_3OH, CH_3CN, HCN, and NH_3.

In this paper, we examine the thermochemistry of hydrogen-bonded clusters containing methanol and water. These clusters

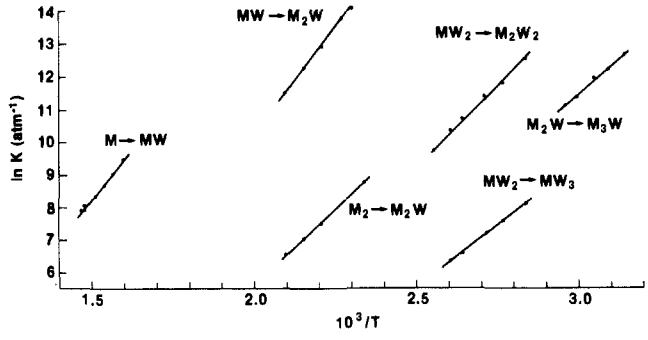

Figure 1. van't Hoff plots for clustering reactions in protonated water–methanol clusters. Formulas indicate the composition of the reactant and product clusters; the proton and the neutral reactants are not shown.

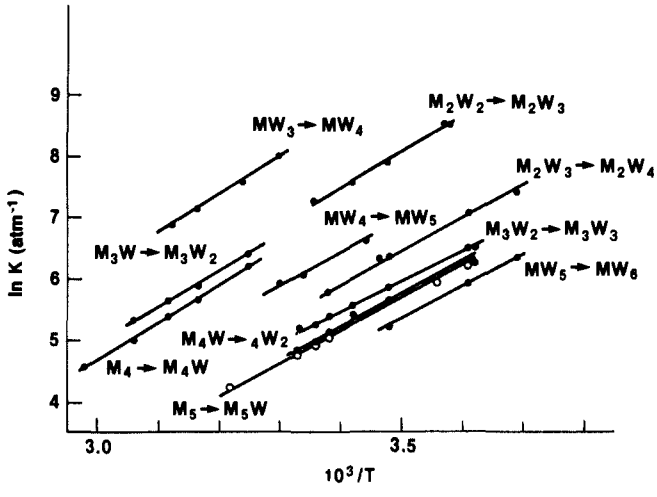

Figure 2. van't Hoff plots for clustering reactions in protonated water–methanol clusters. Notation as in Figure 1.

are models for the soivation of protonated centers in acidic methanol–water solutions and of OH^- or CH_3O^- centers in basic solutions.

To date, multicomponent protonated cluster ions have been examined only in a few systems, which include co-clustering of water with ammonia,[1] hydrogen sulfide,[2] acetonitrile,[3] and dimethyl ether[4] and also methanol–dimethyl ether clusters.[4] The present water–methanol study complements the latter two. As for negative ions, the present study appears to be the first thermochemical study of anionic clusters of mixed solvents.

The present data make it possible for the first time to compare trends in multicomponent cationic clusters vs. anionic clusters of analogous composition. This is of interest because both are bonded by networks of O—H^+···O^- type hydrogen bonds.

An infinite network of efficient OH···O hydrogen bonds is possible in both the cationic and anionic water–methanol clusters. We shall compare these clusters with clusters of water with NH_3 or H_2S, where weaker hydrogen bonds are formed, and with clusters involving MeCN and Me_2O, where hydrogen bonds may be blocked by methyl substitution.

Experimental Section

The measurements were done with the NBS pulsed high-pressure mass spectrometer.[5] For the positive ions that contain 1–4 solvent molecules, CH_4 was used as a carrier gas at total source pressures of 0.3–0.8 Torr, with 0.1–10% H_2O and CH_3OH vapor. For larger clusters, the carrier was neat H_2O with 1–10% CH_3OH vapor. For the negative ion clusters, the carrier gas was CH_4 or cyclohexane with 5% N_2O as electron scavenger. In these alkane–N_2O mixtures the primary ion is O^- which reacts to form OH^- as the reactant ion.[6] In some experiments, the carrier gas

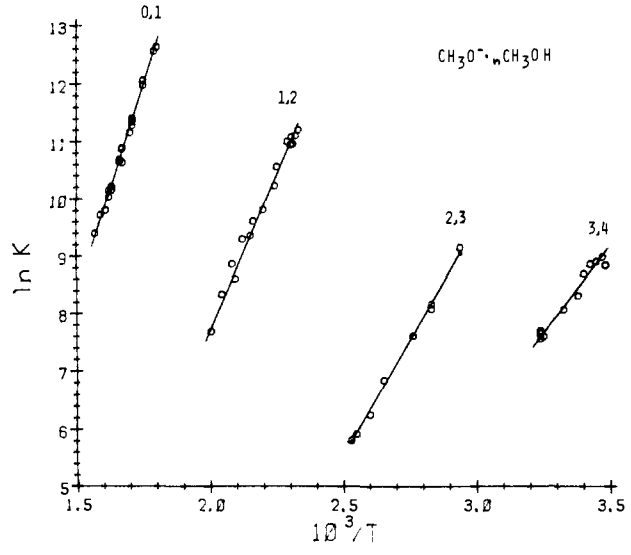

Figure 3. van't Hoff plots for $CH_3O^-\cdot(n-1)CH_3OH + CH_3OH \rightleftharpoons CH_3O^-\cdot nCH_3OH$. $n-1$, n as indicated.

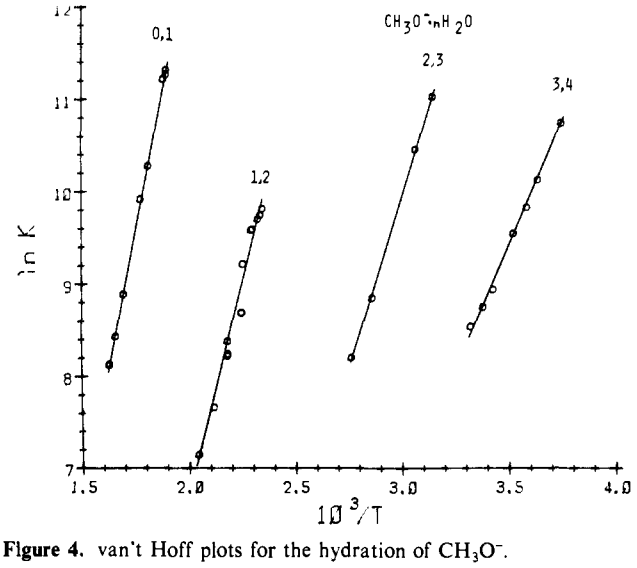

Figure 4. van't Hoff plots for the hydration of CH_3O^-.

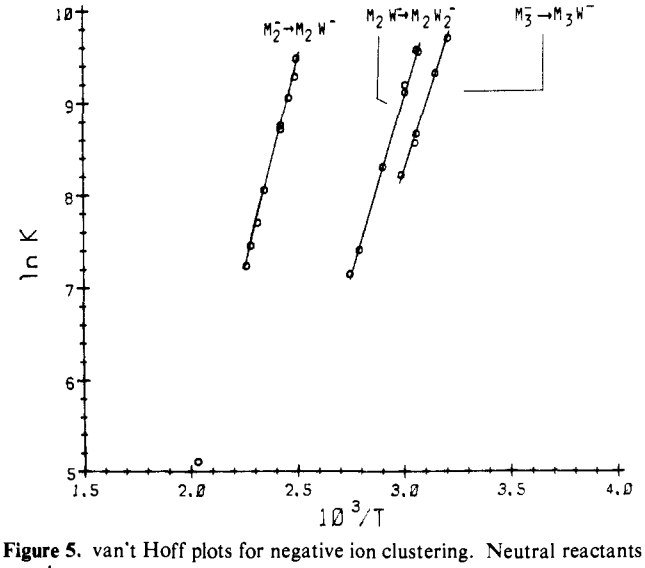

Figure 5. van't Hoff plots for negative ion clustering. Neutral reactants not shown.

(1) Payzant, J. D.; Cunningham, A. J.; Kebarle, P. *Can. J. Chem.* **1973**, *51*, 3242.
(2) Hiraoka, K.; Kebarle, P. *Can. J. Chem.* **1977**, *55*, 24.
(3) Deakyne, C. A.; Meot-Ner (Mautner), M.; Campbell, C. L.; Hughes, M. G.; Murphy, S. P. *J. Chem. Phys.* **1986**, *84*, 4958.
(4) Hiraoka, K.; Grimsrud, E. P.; Kebarle, P. *J. Am. Chem. Soc.* **1972**, *94*, 3359.
(5) Meot-Ner (Mautner), M.; Sieck, L. W. *J. Am. Chem. Soc.* **1983**, *105*, 2956.

Table I. Thermochemistry of Clustering in Water (W) and Methanol (M)[a]

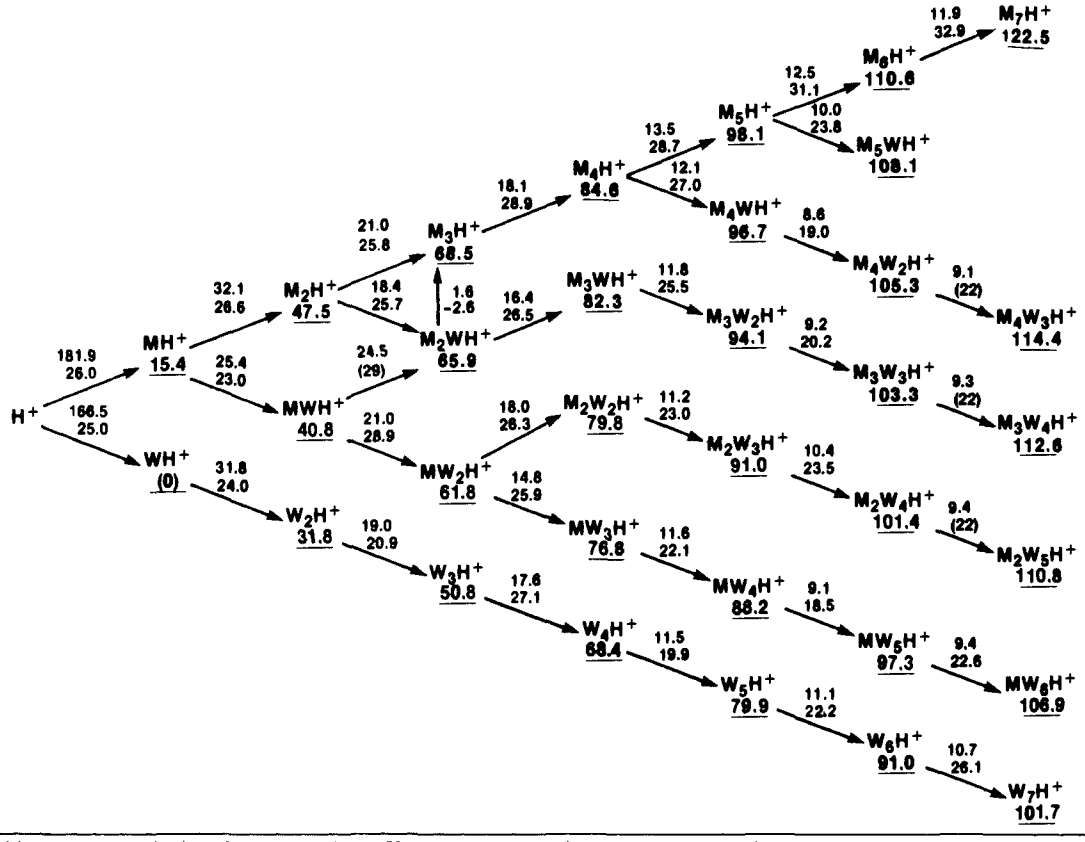

[a] $-\Delta H°$, kcal/mol, (top number) and $-\Delta S°$, cal/(mol·K) (bottom number) over arrows. Numbers under cluster formulas indicate total enthalpy of dissociation to H_3O^+ plus neutrals (for procedure, see Appendix). $\Delta S°$ values in parentheses are estimated; corresponding $\Delta H°$ values are derived from $\Delta G°(T, K)$, kcal/mol values measured at one temperature, as follows: $MWH^+ \rightarrow M_2WH^+$, 11.6 (452); $M_2W_4H^+ \rightarrow M_2W_5^+$, 3.5 (269); $M_3W_3H^+ \rightarrow M_3W_4^+$, 3.2 (272); $M_4W_2H^+ \rightarrow M_4W_3^+$, 3.1 (272). Notation, see Appendix; sources of data, see text.

was neat N_2O. Some other experiments were conducted with CH_4 as the carrier gas with trace CH_3ONO, which yields CH_3O^- after electron capture. CH_3ONO was prepared by the method of Caldwell and Bartmess[7] by mixing a few drops of isoamyl nitrite and methanol and injecting vapor from the headspace in the vial into the heated sample inlet bulb of the mass spectrometer. The total source pressure in the negative ion experimens was 0.8–2.4 Torr, and H_2O and CH_3OH vapor was 1–10% of the total gas mixture. As usual, checks were made to confirm that the equilibrium constant was independent of pressure within the experimental range.

Results

van't Hoff plots for the present equilibria are shown in Figures 1–5, and the thermochemical results are summarized in Tables I–IV. In addition to the present data, included in the tables are recent thermochemical data as follows.

For $H_3O^+ \cdot nH_2O$, the values in Table I are from our recent measurements.[8] These values are in excellent agreement (within ±1 kcal/mol and ±2 cal/(mol·K)) with the most recent set of values by Kebarle et al.[9,10] For $OH^- \cdot nH_2O$, the values are from recent measurements in our laboratory.[8] Here the values agree well with the data of Kebarle et al.[11,12] for the 0,1, 1,2, and 2,3 equilibria, while for the higher equilibria Kebarle's values may be somewhat too high, possibly due to thermal dissociation problems.[13]

For the $CH_3OH_2^+ \cdot nCH_3OH$ clusters, we measured the 0,1 and 1,2 equilibria and found excellent agreement with the results of Kebarle et al.[4] The data for the higher clusters in this system in Table III are quoted from Kebarle et al.[4] For the clusters with $n = 4$–6 (i.e., M_5H^+–M_7H^+ in Table III) the quoted ΔH and ΔS values may be somewhat too large because of thermal dissociation problems that were demonstrated later for other measurements on large clusters.[13] The data for $CH_3OH_2^+ \cdot nH_2O$ are from this laboratory,[14] and the data for $CH_3O^- \cdot nCH_3OH$ and $CH_3O^- \cdot nH_2O$ and the other multicomponent clusters are from the present work.

In terms of standard deviations of the slopes and intercepts of van't Hoff plots, reproducibility of replicate plots, and comparison with Kebarle's data, the error estimate for the present work is ±1 kcal/mol for $\Delta H°$ and ±2 cal/(mol·K) for $\Delta S°$. An exception is the $CH_3O^- \cdot H_2O + H_2O \rightarrow CH_3O^- \cdot 2H_2O$ reaction, where several temperature studies gave an unreasonably small slope, suggesting an artifact. The values for this reaction in Tables III and IV are derived from thermochemical cycles involving the adjacent reactions.

Of primary interest with respect to multicomponent clusters are the relative energies of clusters of various compositions of a given rank r, where r is the total number of solvent molecules $r = m + n$ in the clusters $(CH_3OH)_m(H_2O)_nH^+$ or in $[(CH_3O)_m(H_2O)_n - H]^-$. (This notation for mixed clusters is used to avoid structural inferences and for symmetry of notation between cationic and anionic clusters. See comment on notation in the Appendix.) We express the relative energies of the clusters in terms of the energies needed for the dissociation of the various clusters to the highest energy monomer ion:

$$(CH_3OH)_m(H_2O)_nH^+ \rightarrow H_3O^+ + mCH_3OH + (n-1)H_2O$$

$$((CH_3OH)_m(H_2O)_n - H)^- \rightarrow OH^- + mCH_3OH + (n-1)H_2O$$

(6) Smit, A. L. C.; Field, F. H. *J. Am. Chem. Soc.* **1977**, *99*, 6471.
(7) Caldwell, G.; Bartmess, J. E. *Org. Mass Spectrom.* **1982**, *17*, 456.
(8) Meot-Ner (Mautner), M.; Speller, C. V. *J. Phys. Chem.*, in press.
(9) Cunningham, A. J.; Payzant, J. D.; Kebarle, P. *J. Am. Chem. Soc.* **1972**, *94*, 6267.
(10) Lau, Y. K.; Ikuta, S.; Kebarle, P. *J. Am. Chem. Soc.* **1982**, *104*, 1462.
(11) Arshadi, M.; Kebarle, P. *J. Phys. Chem.* **1970**, *74*, 1463.
(12) Payzant, J. D.; Yamdagni, R.; Kebarle, P. *Can. J. Chem.* **1971**, *49*, 3308.
(13) Sunner, J.; Kebarle, P. *J. Phys. Chem.* **1981**, *85*, 327.
(14) Meot-Ner (Mautner), M. *J. Am. Chem. Soc.* **1984**, *106*, 1265.
(15) Newton, M. D.; Ehrenson, S. *J. Am. Chem. Soc.* **1971**, *93*, 4971.
(16) Meot-Ner (Mautner), M. In *Structure–Energy Relations*; Liebman, J. L., Greenberg, A., Eds.; Springer-Verlag: New York, 1986, in press.

Table II. Free Energies of Clustering[a]

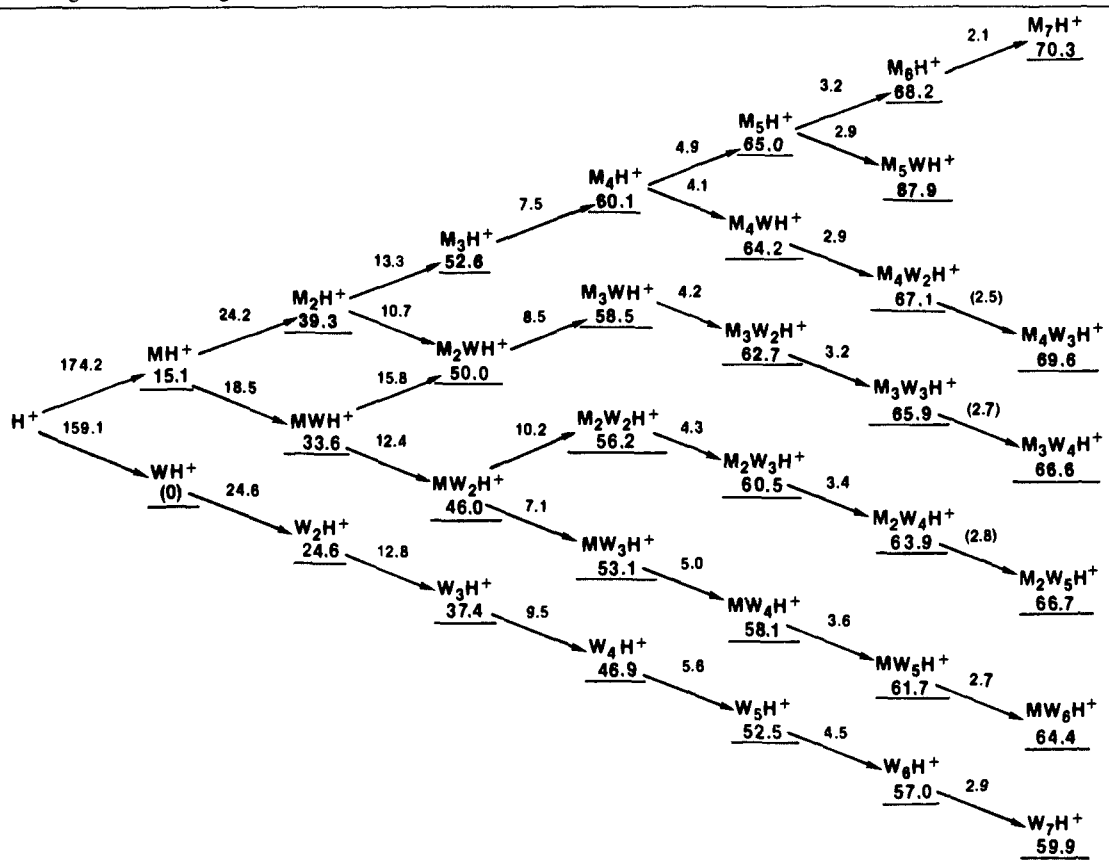

[a] $-\Delta G°(300) = -\Delta H° + 300\Delta S°$, kcal/mol, using experimental $\Delta H°$ and $\Delta S°$ values from Table I. Notation as in Table I.

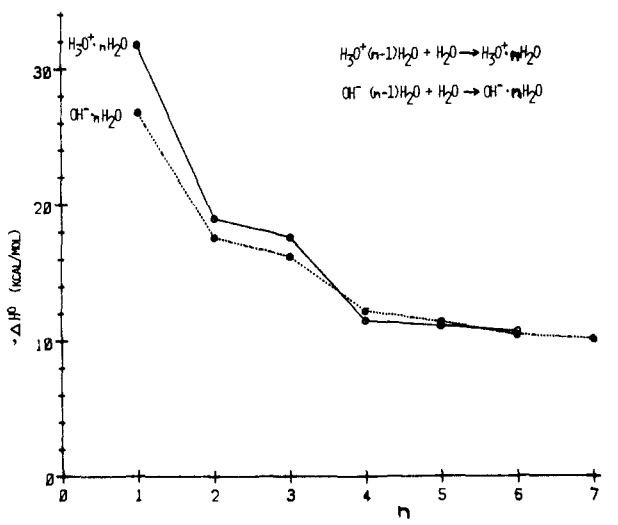

Figure 6. Enthalpy sequence, i.e., $-\Delta H°_{n-1,n}$ vs. n for the hydration of H_3O^+.

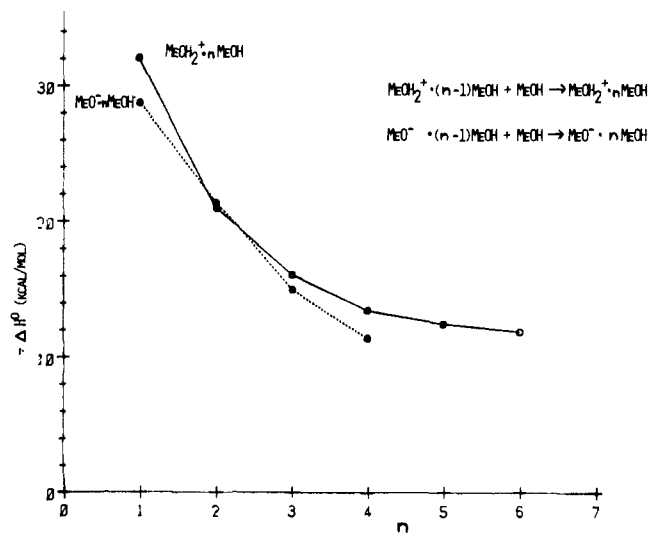

Figure 7. Enthalpy sequence for the addition of CH_3OH molecules to $CH_3OH_2^+$ and CH_3O^-.

Note that in the case of neat methanol clusters, the analogous energetics to yield H_3O^+ or OH^- also involve proton transfer. These dissociation energies are presented under each cluster in Tables I–IV. When a cluster can be reached by several ways through cycles, the dissociation energies given are the average obtained from the various cycles. The procedure is described in the Appendix.

The next section will examine the enthalpy sequences in the neat and hydrated clusters, i.e., $-\Delta H°_{n-1,n}$ vs. n. The rest of the discussion will be given mostly in terms of free energies. However, inspection of Tables I–IV shows that the enthalpies exhibit the same trends as the free energies. The use of free energies is preferred because these values are more accurate than enthalpies when long extrapolations to 300 K are not needed. Free energies are also of direct interest in terms of equilibrium cluster distributions.

Discussion

1. The Stepwise Buildup of Clusters. The enthalpy sequences for the consecutive addition of neutrals to the cluster, reactions 1–4, are shown in Figures 6–8. Here B = water (W) or methanol

$$B_{n-1}H^+ + B \rightleftarrows B_nH^+ \quad (1)$$

$$(B_{n-1} - H)^- + B \rightleftarrows (B_n - H)^- \quad (2)$$

$$MeOH_2^+ \cdot (n-1)H_2O + H_2O \rightleftarrows MeOH_2^+ \cdot nH_2O \quad (3)$$

$$MeO^- \cdot (n-1)H_2O + H_2O \rightleftarrows MeO^- \cdot nH_2O \quad (4)$$

Table III. Thermochemistry ($\Delta H°$ and $\Delta S°$) of Clustering in Water–Methanol[a]

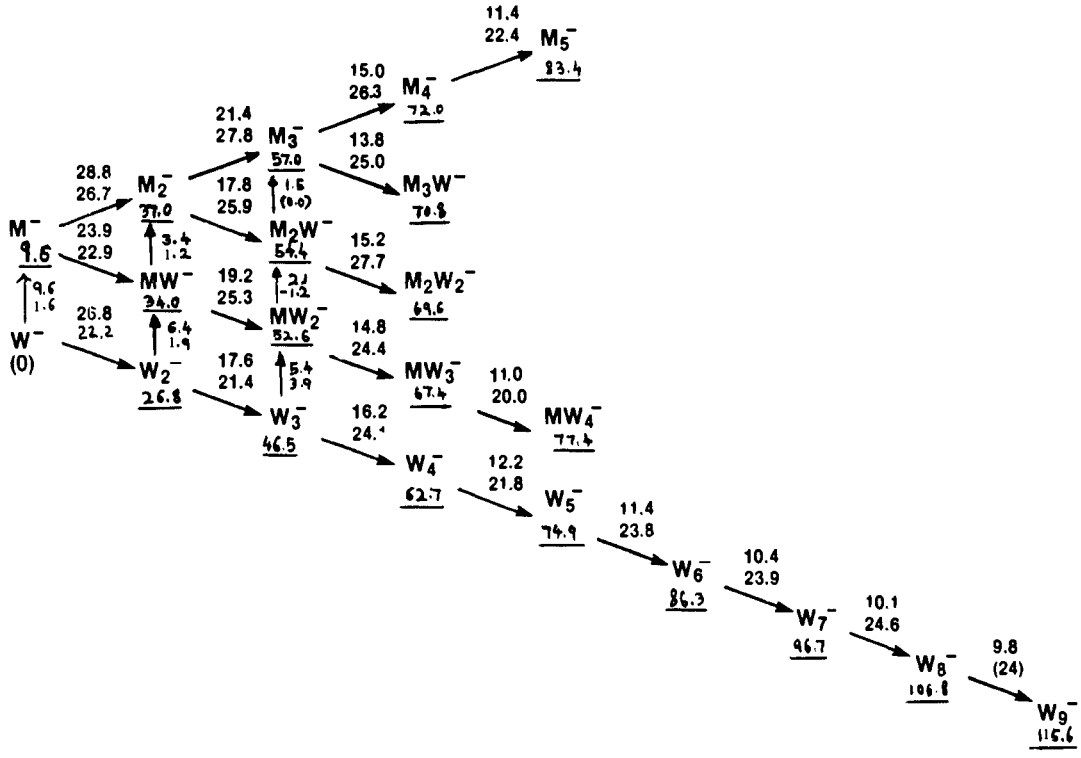

[a] $W_mM_n^-$ is shorthand for $((H_2O)_m(CH_3OH)_n - H)^-$. For $M_2^- \rightarrow M_3^-$, $\Delta S°$ is estimated; $\Delta H°$ derived from $\Delta H°(344) = -1.5$ kcal/mol. Notation, see Appendix; sources of data, see text.

Table IV. Free Energies of Clustering[a]

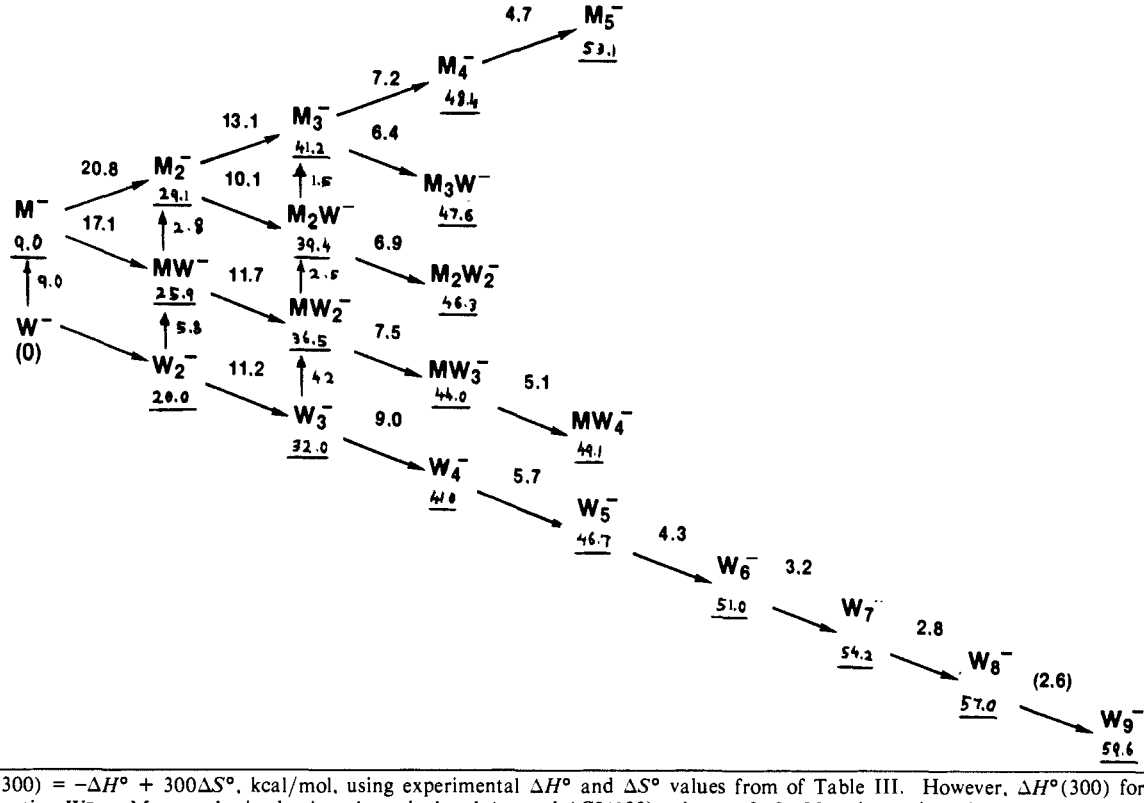

[a] $-\Delta G°(300) = -\Delta H° + 300\Delta S°$, kcal/mol, using experimental $\Delta H°$ and $\Delta S°$ values from of Table III. However, $\Delta H°(300)$ for the proton transfer reaction $W^- \rightarrow M^-$ was obtained using also calculated Δc_p and $\Delta S°(300)$ values, ref 19. Notation as in Table III.

(M). Reactions 1 and 2, with B = H_2O or MeOH, constitute the buildup of neat clusters, and reactions 3 and 4 are the hydration of $MeOH_2^+$ and MeO^-, respectively. As usual, $-\Delta H°_{n-1,n}$ decreases with increasing n for all the clusters, as the charge becomes increasingly diffuse in the clusters. The patterns of the variation of $\Delta H°_{n-1,n}$ with n, i.e., of the enthalpy sequences, are somewhat different in the neat water, neat methanol, and hydrated methanol clusters (Figures 6–8). However, in each system, the enthalpy sequences in the corresponding positive and negative ion cluster are remarkably similar. In all three cases, the $\Delta H°$ for the 0,1 equilibria of the negative ions, which involve $OH^-\cdots O$ bonds, is lower by 2–5 kcal/mol than the corresponding $OH^+\cdots O$ hydrogen

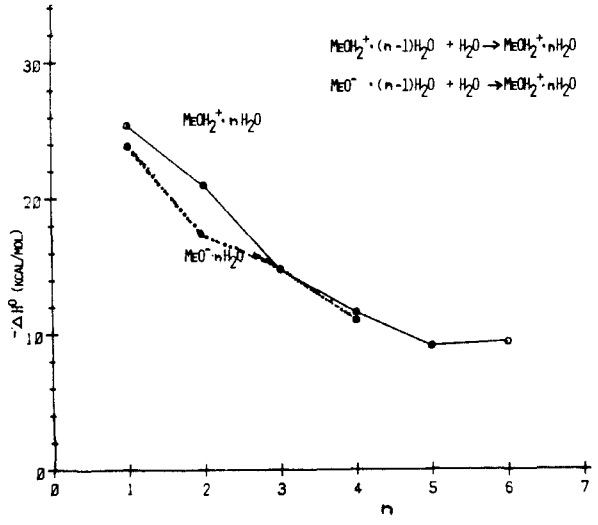

Figure 8. Enthalpy sequence for the hydration of $CH_3OH_2^+$ and CH_3O^-.

bonds. In all three systems, the differences between the positive and negative ion clustering energies decrease with increasing n. An apparent deviation from this for $n = 4$ in the neat methanol clusters may be due to erroneously high values in the positive clusters from ref 4, as noted above.

A particularly notable similarity is found between the enthalpy sequences of $H_3O^+\cdot nH_2O$ and $OH^-\cdot nH_2O$ (Figure 6), both of which show a break after $n = 3$. In H_3O^+ this is obviously associated with shell filling, as in ion **1**. In OH^- the reason for shell filling is less obvious. However, Newton and Ehrenson[15] showed that the most stable isomer of $OH^-\cdot 3H_2O$ is ion **2** where three lone pairs of OH^- are occupied by hydrogen bonds. Therefore, in the anionic cluster the fourth water molecule must add in an outer shell, as is the case also, for other reasons, in the cationic cluster.

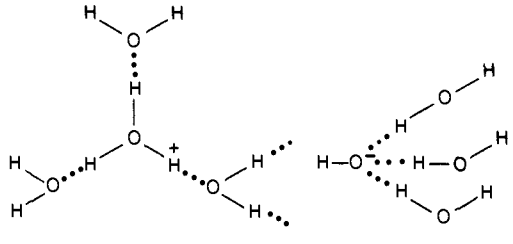

1 **2**

A shell-filling effect is also seen in $MeOH_2^+\cdot 2H_2O$. Inspection of the van't Hoff plots suggests possible small shell-filling effects also in $MeO^-\cdot 3H_2O$. However, these effects are within the error limits of the measurements.

2. The Relative Energies of the Neat Clusters. The Solvation of the Proton in Neat Solvents. The total bonding energies of clusters of neat B vs. neat water clusters are given by the energy of reaction 5 and the analogous reaction 6 for negative ions.

$$(H_2O_n)H^+ + nB \rightleftarrows B_nH^+ + nH_2O \quad (5)$$

$$((H_2O)_n - H)^- + nB \rightleftarrows (B_n - H)^- + nH_2O \quad (6)$$

For $n = 1$, ΔG for reaction 5 is the difference between the gas phase basicities of H_2O and B. For increasing n, ΔG reflects the relative stabilization of the proton by increasing solvation by B vs. H_2O.

In the mixed clusters of MeOH, Me_2O, and MeCN with H_2O, the larger component stabilizes the charge more than H_2O. Therefore, for all the clusters observed, $\Delta G°_5$ is negative. However, $\Delta G°_5$ becomes less negative as n increases (Figure 9), because water is a more efficient hydrogen-bonding solvent than any of the other compounds.

Indeed, the trends in transfering the proton from water to other solvent clusters in Figure 9 seem to be determined primarily by hydrogen-bonding effects. Thus, transfer to ammonia becomes

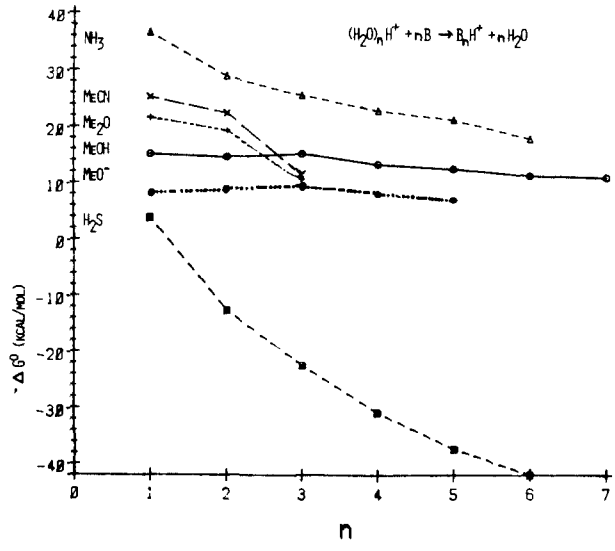

Figure 9. Free energies for proton transfer from $(H_2O)_n$ to B_n. For MeO^-, reaction 6, see text.

increasing less exoergic as increasingly larger hydrogen-bonding networks in water are substituted by weaker ammonia networks. The effect is even more pronounced in transfer to the weakly hydrogen bonding H_2S, where for $n = 2$ the transfer already becomes endoergic. Also reflected in Figure 9 is the blocking of hydrogen bonding after $n = 2$ for MeCN and Me_2O.

Somewhat surprisingly, however, the plot for transfering the proton from water to methanol shows only a slight decrease in exoergicity with n. Of course, MeOH as well as H_2O is capable of forming an infinite network of OH···O type hydrogen bonds, though in MeOH half the sites are blocked. The trend in Figure 9 shows that this partial blocking has only a slight effect on the solvation of the proton. A similar trend is observed for the anionic clusters (the line corresponding to MeO^- in Figure 9). In the anion clusters too, infinite hydrogen-bonding networks are possible both in $OH^-\cdot nH_2O$ and in $CH_3O^-\cdot nCH_3OH$. Therefore, replacing nH_2O by nCH_3OH as a solvent seems to have little effect in stabilizing the negative charge.

The differences between the total dissociation energies of each $H_3O^+\cdot nH_2O$ are higher than of $OH^-\cdot nH_2O$ by a constant 5 ± 1 kcal/mol, for $n = 1$–6 (Tables I and III). This shows that the difference between the total dissociation energies of the cationic vs. anionic neat water clusters arises from the difference between the strengths of the first OH^+···O vs. OH···O^- bond in these clusters. A similar difference is noted also between the hydrogen bonds in $CH_3OH_2^+\cdot CH_3OH$ vs. $CH_3O^-\cdot CH_3OH$. However, here the difference diminishes in the higher clusters, possibly due to erroneously high values for the cationic methanol clusters, as noted above.

The general observation is then that positive hydrogen-bonded networks are more stable than the corresponding negative hydrogen-bonded networks by about 3–6 kcal/mol. This difference arises primarily from the first O—H^+···O and O—H···O^- hydrogen bonds in the positive and negative dimers, respectively.

3. Transfer of Proton with Its Hydration Shell. Effects of Hydration on Basicities and Acidities. From clustering data, it is possible to calculate the thermochemistry for the transfer of a proton along with a solvent shell, reactions 7 and 8. For $n = 0$, $\Delta G°_7$ and $\Delta G°_8$ express the differences between the gas-phase basicities or acidities of H_2O and B, respectively.

$$H_3O^+\cdot nH_2O + B \rightleftarrows BH^+\cdot nH_2O + H_2O \quad (7)$$

$$OH^-\cdot nH_2O + CH_3OH \rightleftarrows CH_3O^-\cdot nH_2O + H_2O \quad (8)$$

The variation of $\Delta G°_7$ with n shows the effects of increasing ion solvation on the acidities or basicities of B vs. H_2O (the effects of the solvation of the neutral B vs. H_2O on the basicities is not included). Figure 10 shows the well-known result that increasing solvation tends to compress the differences between the gas-phase

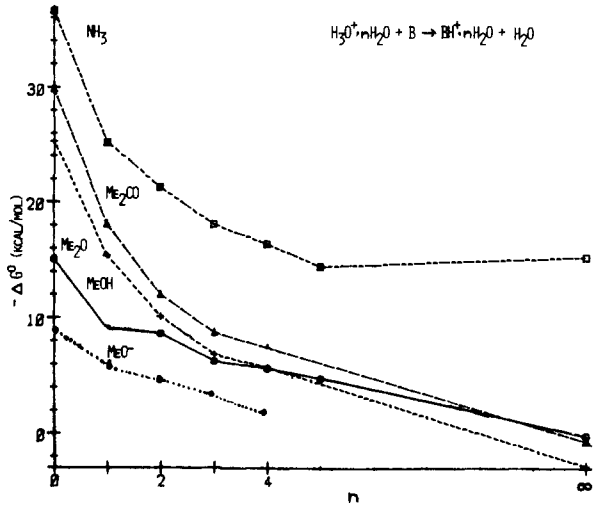

Figure 10. Free energies for the transfer of proton and n water molecules from H_2O to B, reaction 7. For CH_3O^-, the analogous reaction 8, see text.

basicities of compounds, since ions BH^+ of weaker bases are stabilized by solvation more efficiently than of stronger bases. For the oxygen bases in Figure 10, the values and the spread of the values of $\Delta G°_7$ are decreased from 15–30 kcal/mol for $n = 0$ to 6–9 kcal/mol for $n = 4$. However, further decreases in the relative basicities of the alkylated compounds vs. H_2O and NH_3 occur in going from the clusters to aqueous solution ($n = \infty$ in Figure 10), probably due to the less efficient aqueous hydration of the large, blocked alkylated ions. The detailed effects of the cavity, dielectric, hydrophobic, and ionic hydrogen bonding energies in the hydration of alkylated ions are analyzed elsewhere.[17]

Figure 10 also shows that the effects of gradual ion hydration on the relative basicities of H_2O and CH_3OH are approximately comparable to the effects on the relative acidities (i.e., the lines labeled MeOH and MeO^- in Figure 10 are approximately parallel). Here, however, the more efficient hydration of H_3O^+ vs. $CH_3OH_2^+$ has a larger effect (the difference in basicities decreases from 15.1 to 5.6 kcal/mol for $n = 4$) than the hydration of OH^- vs. CH_3O^- (the difference in acidities is reduced from 8.7 to 3.0 kcal/mol for $n = 4$).

$-\Delta G°_8(298)$ was measured by flowing afterglow technique by Mackay and Bohme.[18] Their results agree with the present data in that $-\Delta G°_8$ decreases with increasing n. Their $-\Delta G°_8(298)$ values for $n = 1$, 2, and 3 are >4.3, 3.0, and 1.9 kcal/mol, respectively, in reasonable agreement with our 5.8, 4.5, and 3.0 kcal/mol, respectively. Reasonable agreement is also found for the reactions (in the notation of Table I) $MW^- \rightarrow M_2^-$ and $MW_2^- \rightarrow M_2W^-$, where the flowing afterglow results are 2.0 and 2.0 kcal/mol, respectively, compared with the present results of 3.7 and 2.1 kcal/mol, respectively.

Equations 7 and 8 and the trends in Figure 10 do not involve the hydration of the neutral reactants. Extrapolation to n = infinity expresses the effects of ion hydration alone on the relative basicities of B vs. H_2O. However, to consider the total solvation effects on relative basicities, the solvation of the neutral bases must also be included, and the pertinent clustering equation is eq 9, rather than eq 7. Equation 9 takes into account the clustering

$$H_3O^-\cdot nH_2O + B\cdot nH_2O \rightleftarrows BH^+\cdot nH_2O + H_2O\cdot nH_2O \quad (9)$$

of the neutral bases. However, the neutral clustering energies are not well known. Also, from the point of view of ion chemistry, the effects of ion solvation alone are of more direct interest. Therefore for trend analysis in ion chemistry, the use of reaction 7, rather than reaction 9, is more accurate and pertinent.

With respect to the acidity difference between unclustered gaseous H_2O and CH_3OH, the values in Tables III and IV are

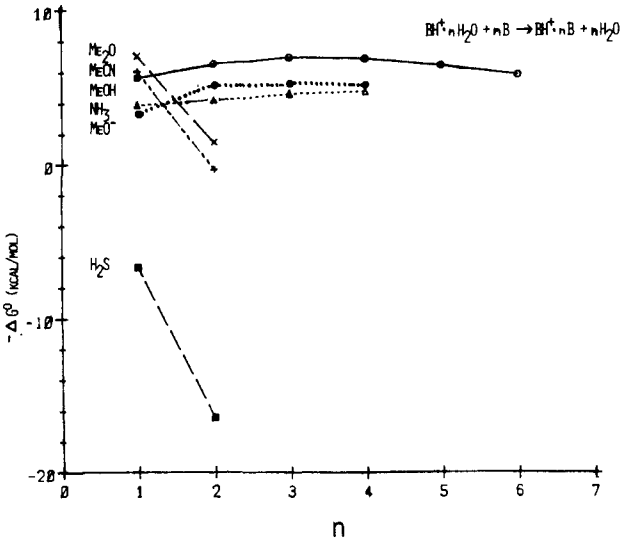

Figure 11. Free energies for the transfer of BH^+ from $n H_2O$ to nB, reaction 10. For CH_3O^-, the analogous reaction 11, see text.

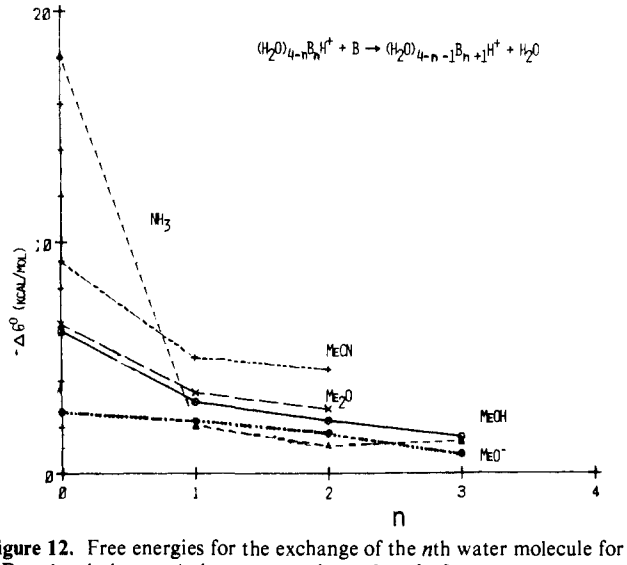

Figure 12. Free energies for the exchange of the nth water molecule for a B molecule in $r = 4$ clusters, reactions 12 and 13, see text.

8.7 kcal/mol from our measurements,[19] smaller than the currently accepted value of 11.5 kcal/mol,[20] as will be discussed elsewhere.[19]

4. Clustering of BH^+ by nB vs. $n H_2O$. The transfer of the proton from water clusters to B_n clusters, reaction 5, can be decomposed into two steps: the transfer of the proton along with its hydration shell to B, reaction 7, followed by an exchange of solvent shells, reaction 10. For the anions, the analogous reactions are reactions 6, 8, and 11, respectively. Somewhat unexpectedly,

$$BH^+\cdot nH_2O + nB \rightleftarrows BH^+\cdot nB + nH_2O \quad (10)$$

$$MeO^-\cdot nH_2O + n\text{MeOH} \rightleftarrows MeO^-\cdot n\text{MeOH} + nH_2O \quad (11)$$

Figure 11 shows that for solvents that can form unlimited hydrogen bonded networks, i.e., NH_3 and MeOH, the solvation of the ions in the neat clusters is more exergonic by 4 and 6 kcal/mol, respectively, than solvation by water clusters, and the difference is nearly independent of the increasing cluster size n. This also applies for the solvation of MeO^- by nMeOH vs. nH_2O, and the trend again parallels that of the respective positive ions. In contrast, in the case where hydrogen bonding is blocked, or inefficient as in H_2S, reaction 10 becomes rapidly less exergonic at $n = 2$ (Figure 11).

5. The Stepwise Substitution of H_2O Molecules by B. For the relative stabilities of clusters of a given rank r, it is of interest to

(17) Meot-Ner (Mautner), M. *J. Phys. Chem.*, in press.
(18) Mackay, G. I.; Bohme, D. K. *J. Am. Chem. Soc.* **1978**, *100*, 327.
(19) Meot-Ner (Mautner), M.; Sieck, L. W. *J. Phys. Chem.*, in press.
(20) Bartmess, J., private communication.

examine the effect of the stepwise replacement of water molecules by the other component, B. The reactions are written formally as reactions 12 and 13. We examine the trends in clusters of

$$(H_2O)_{r-n}B_nH^+ + B \rightleftarrows (H_2O)_{r-n-1}B_{n+1}H^+ + H_2O \quad (12)$$

$$[(H_2O)_{r-n}B_n - H]^- + B \rightleftarrows [(H_2O)_{r-n-1}B_{n+1} - H]^- + H_2O \quad (13)$$

rank $r = 4$, the largest where data for the anions are available. Figure 12 shows that the largest effect in all the clusters is for $n = 0$, i.e., for the introduction of the first B molecule into the cluster. This is understandable, since this step involves proton transfer from H_2O to B, and the proton affinities of all of the molecules B in Figure 12 are larger than those of H_2O. However, further exchanges of H_2O for **B** remain exergonic for all the steps and all of the B molecules, until the neat BH^+ or $(B - H)^-$ cluster is reached. Exceptions are MeCN and Me_2O, where the neat B_4H^+ clusters are blocked against hydrogen bonding.

In H_2O–MeCN clusters we observed that the most stable cluster of each rank is the one containing the largest number of the nonaqueous, high proton affinity component which still allows all molecules to attach to the cluster by strong OH···O or NH···O hydrogen bonds.[3] This rule also applies to all the bases B in Figure 12. In the H_2O–MeOH clusters an infinite number of MeOH molecules can be added without blocking further hydrogen bonding. Therefore, the above rule simply states that the most stable cluster of each rank is the neat methanol cluster. This applies also in the case of the negative ion clusters.

Conclusion

The present results allow the comparative examination of positive and negative ion clusters bonded by O—H···O hydrogen bond networks. In the variation of cluster stabilities with rank r and composition, the negative and positive ion clusters show remarkable similarities. In several respects, the trends in both the positive and negative water–methanol clusters are different from clusters in which weaker hydrogen bonds involving NH_3 or H_2S are involved. The water–methanol clusters, where unlimited networks of strong H—O···H hydrogen bonds are possible, are also different from those water–MeCN and water–Me_2O clusters which are destabilized by the blocking of the hydrogen bonds.

While the trends in cluster stability vs. composition are similar in the positive and negative ion clusters, the overall stabilization of each positive ion cluster, with respect to dissociation to the most stable monomer ion, is greater by 3–6 kcal/mol than the corresponding negative cluster. The difference between the stabilities of the positive vs. negative ion hydrogen bonded networks arises primarily from the first O—H^+···O vs. O—H···$^-$O bond as reflected in the dimer ions.

In both the anionic and cationic clusters, increasing methanol content always stabilizes the cluster. This suggests that in mixed water–methanol solutions in H^+ or an RO^- center will be solvated preferentially by methanol molecules. The result also suggests that methanol and possibly other small alcohols are better solvents than water for H^+ and RO^-.

In terms of the topology of cluster conformation, these observations suggest that in mixed water–methanol clusters, the most stable isomers will have the methanol molecules near the charged center. This is opposite to water–acetonitrile and water–dimethyl ether clusters. In water–acetonitrile, it was suggested[4] and later shown by ab initio calculations[3] that the most stable isomers have water in the center, in order to allow for a network of strong O—H···O and N—H···O or O—H···N hydrogen bonds. Therefore, despite the large difference in the proton affinities of H_2O and MeCN, the proton is located on the water in, for example, the $H_3O^+ \cdot 3MeCN$ (ion **3**) and probably on the $H_5O_2^+$ moiety in $(H_2O)_2(MeCN)_4H^+$, pushing the MeCN molecules to the periphery. In contrast, the present results suggest that in water–methanol clusters, the methanol molecules are near the charged center ion. For example, ion **4** should be more stable than ion **5** and the water is at the periphery of the cluster. However, clusters grow by attachment to hydrogen, and H_3O^+ in the center

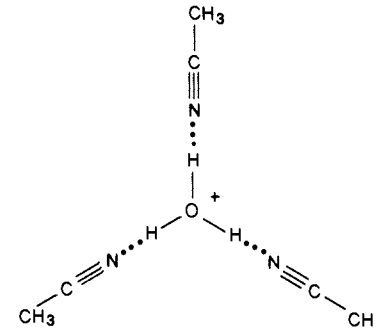

3

allows branched structures which place more molecules near the charged center. This allows more stabilization for branched structures,[3,15] and therefore the difference between **4** and **5** may be small, and both isomers may be present in equilibrium.

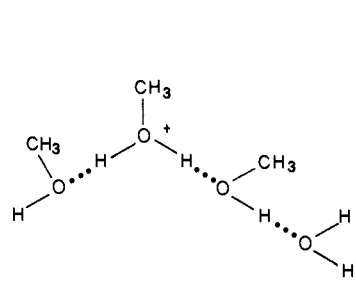

4

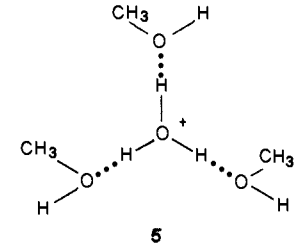

5

In the anion clusters, there is a clearer advantage to place methanol molecules near the charged center as in ion **6**. Here clusters grow by attachment of neutrals to oxygen lone pairs, and since both H_2O and MeOH have two pairs, alternative structures such as I still cannot place more molecules near the charged center.

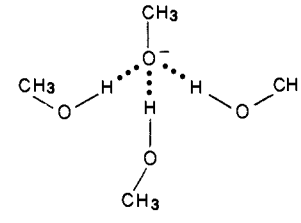

6

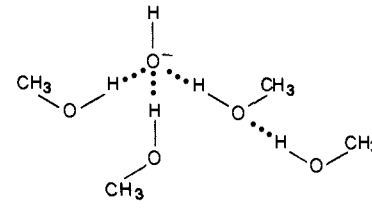

7

In summary, this work allows the first comparison of cationic and anionic hydrogen-bonded networks of mixed clusters. The stability trends in cationic and anionic water–methanol clusters are similar, and both demonstrate the importance of the formation of unlimited O—H···O hydrogen-bonded networks.

Appendix

1. A Procedure for Assigning Stabilities from Clustering Networks. In networks such as in Tables III and IV, the stabilities of the clusters of rank 2 and 3 vs. dissociation to the reference monomer OH^- ion can be derived from several alternative paths. This is a general situation for mixed clusters, and a standard procedure to assign average total stability values is desirable.

In the present work the following procedure is adopted. The stability of each cluster of rank r is calculated on the basis of the stability of clusters of rank $r - 1$. In each path used, the first step

proceeds from a cluster of rank $r - 1$ to a cluster of rank r; in this manner, only the already evaluated best stability of each cluster of rank $r - 1$ is used to assign values to the next rank clusters.

For example, for M_2W (sign of charge omitted) we use $W_2 \rightarrow W_3 \rightarrow MW_2 \rightarrow M_2W$; $MW \rightarrow MW_2 \rightarrow M_2W$; $M_2 \rightarrow M_2W$ and $M_2 \rightarrow M_3 \rightarrow M_2W$. However, for example, $MW \rightarrow M_2 \rightarrow M_2W$ is not used, since the first step here connects clusters whose relative stabilities were already assigned, and using the directly measured value for the $MW \rightarrow M_2$ reaction would overemphasize the weight of this measurement in building up the next column.

The n paths reaching a cluster of rank r from the rank $r - 1$ clusters give n values for ΔG_{total} for that cluster. Each of these n values is assigned a random error, which is the propagated error associated with the precursor cluster and of the steps used in that particular path. A weighted least-squares average of these n values for the given cluster is assigned as the chosen value. Note that the weighted averaging allows less influence by values derived from long paths, since these have larger propagated errors.

2. Notes on Terminology. The total number of components in a cluster is often denoted as "cluster size". This may be misleading, however, since clusters with the same number of monomers may differ greatly in size; and a "smaller cluster" $(CH_3OH)_4$ is larger in physical size thn a "larger cluster" $(H_2O)_6$. Above, the term "rank r" was used to avoid this ambiguity.

In the present paper, mixed clusters are denoted as $(CH_3OH)_m(H_2O)_nH^+$ and $((CH_3OH)_m(H_2O)_n - H)^-$. The notation is somewhat inconvenient, especially for the anions. However, alternative notations would imply structures that are not always predictable. For example, for $(CH_3CN)(H_2O)_3H^+$, the intuitive structure would be $CH_3CNH^+ \cdot 3H_2O$, while ab initio calculations show $H_3O^+ \cdot 2H_2O \cdot CH_3CN$. Therefore, notation such as $CH_3O^- \cdot mCH_3OH \cdot nH_2O$ should be avoided. Another, somewhat more accurate alternative, such as $((CH_3OH)_m(H_2O)_n - H^+)$ to denote the deprotonated anion clusters would also be confusing. A further advantage to the present notation is that it is symmetric for anionic and cationic clusters of similar composition.

A shorthand notation such as $M_mW_n^-$ is used in Figure 5 and Tables III and IV. For example, $M_2W_2^- = [(MeOH)_2(H_2O)_2 - H]^- = MeO^- \cdot MeOH \cdot H_2O$, etc. $M_mW_n^-$ as used here should not be confused with the radical anion $[(CH_3OH)(H_2O)]^{\bullet -}$.

Registry No. CH_3OH, 67-56-1.

The Effects of Chloro Substitution on the Electronic Structure of $ClCr^+$, $ClMn^+$, and $ClFe^+$ and Their Reactivity with Small Alkanes

M. L. Mandich,* M. L. Steigerwald,* and W. D. Reents, Jr.*

Contribution from AT&T Bell Laboratories, Murray Hill, New Jersey 07974.
Received February 10, 1986

Abstract: The exothermic reactions of $ClCr^+$, $ClMn^+$, and $ClFe^+$ with small alkanes in the gas phase have been investigated in the ion trap of a Fourier transform mass spectrometer. $ClFe^+$ is unreactive. In the $ClMn^+$ reactions, the chlorine radical is displaced, yielding Mn^+-(alkane) products. $ClCr^+$ activates C-C and C-H bonds of the alkanes leading to $ClCr^+$-(alkene) products resulting from loss of H_2 or CH_4. The reactivity of $ClCr^+$ is particularly unusual since ground-state Cr^+ does not react exothermically with small alkanes. A description of the metal-to-chlorine bond has also been obtained with ab initio Hartree-Fock and generalized valence bond calculations. These calculations show that $ClMn^+$ and $ClFe^+$ have a covalent bond between the Cl and the metal which is in the σ space between the two nuclei. An unusual situation occurs in the case of $ClCr^+$ where two bonding configurations are close in energy. One has a covalent σ bond as in $ClMn^+$ and $ClFe^+$. The other has a covalent bond in the π space between the nuclei with the σ space supporting strong donor/acceptor bonding between a doubly occupied Cl orbital and the empty valence s space on the metal. This peculiar bond permits the $ClCr^+$ to act as a diradical species which explains its unexpected reactivity.

Studies of the reactions of coordinatively unsaturated metal ions in the gas phase have revealed rich and unprecedented chemistry at single transition-metal centers. Perhaps the most striking feature of this reactivity is that these metal ions are capable of exothermically activating the relatively inert C-C and C-H bonds of saturated hydrocarbons. This reactivity has been investigated for the atomic metal ions, and extensive information is now available for the first-row transition metals and many of the second-row transition metals.[1-8] Nonetheless, since these metal ions have no ligands, direct comparisons cannot necessarily be made with the large body of knowledge about homogeneous organometallic systems. Therefore, much will be learned about the differences in reactivity and thermochemistry between the gaseous atomic metal ions and corresponding solution-phase organometallic molecules by examining intermediate prototypes such as partially coordinated metal ions. There have been a few studies of partially ligated metal ions, e.g., several $(C_5H_5)M^+$,[9] MH^+,[10] MD^+,[11] MCH_3^+,[12] and MCO^+[13] ions as well as FeO^+[14] and $TiCl_n^+$.[15] Currently, however, reactivities of the coordinated species are much less well described than for the bare metal ion analogues. In this work, we report the reactions of the series $ClCr^+$, $ClMn^+$, and $ClFe^+$ with small alkanes. The reactivity for $ClCr^+$ is particularly unusual. Whereas Cr^+ does not react exothermically with small alkanes, $ClCr^+$ does. This is the first demonstration that addition

(1) Muller, J. *J. Adv. Mass. Spectrum.* **1976**, *68*, 823.
(2) Allison, J.; Freas, R. B.; Ridge, D. P. *J. Am. Chem. Soc.* **1979**, *101*, 1332.
(3) Larson, B. S.; Ridge, D. P. *J. Am. Chem. Soc.* **1984**, *106*, 1912.
(4) Armentrout, P. B.; Beauchamp, J. L. *J. Am. Chem. Soc.* **1980**, *102*, 1736.
(5) Houriet, R.; Halle, L. F.; Beauchamp, J. L. *Organometallics* **1983**, *2*, 1818.
(6) Tolbert, M. A.; Beauchamp, J. L. *J. Am. Chem. Soc.* **1984**, *106*, 8117.
(7) Byrd, G. D.; Burnier, R. C.; Freiser, B. S. *J. Am. Chem. Soc.* **1982**, *104*, 3565.
(8) Jacobson, D. B.; Freiser, B. S. *J. Am. Chem. Soc.* **1983**, *105*, 5197.
(9) Beauchamp, J. L.; Stevens, A. E.; Corderman, R. R. *Pure Appl. Chem.* **1979**, *51*, 967.
(10) Halle, L. F.; Klein, F. S.; Beauchamp, J. J. *J. Am. Chem. Soc.* **1984**, *106*, 2543.
(11) Carlin, T. J.; Sallans, L.; Cassady, C. J.; Jacobson, D. B.; Freiser, B. S. *J. Am. Chem. Soc.* **1983**, *105*, 6321.
(12) Jacobson, D. B.; Freiser, B. S. *J. Am. Chem. Soc.* **1984**, *106*, 3891.
(13) Freas, R. B.; Ridge, D. P. *J. Am. Chem. Soc.* **1980**, *102*, 7129.
(14) Jackson, T. C.; Jacobson, D. B.; Freiser, B. S. *J. Am. Chem. Soc.* **1984**, *106*, 1252.
(15) Allison, J.; Ridge, D. P. *J. Am. Chem. Soc.* **1977**, *99*, 35.

0002-7863/86/1508-6197$01.50/0